

Theoretical Modeling of Resonant Modes of Composite Ultrasonic Transducers

Yongan Shui, Xuechang Geng, and Q. M. Zhang

Abstract—Although a great deal of effort has been devoted to the modeling of composite piezoelectric materials, most of the earlier works are based on the assumption that the structure of the composite relative to the wavelength is very fine. Such approximation cannot address the complete dynamic behavior of composites. In order to understand the overall characteristics of composite ultrasonic transducers, a dynamic model was developed, in which the acoustic waves propagating in 2-2 composites along the thickness direction were analyzed by solving the coupled elastic equations of the constituent phases. By neglecting the boundary conditions of the free surfaces and simply taking the resonator thickness as half a wavelength, the resonant modes of the composite transducers as functions of aspect ratio of the ceramic plate elements and volume fraction of ceramic phase can be calculated from this model. The theoretical dispersion curves for the thickness mode and the lateral periodical mode agree with the experimental results. The vibration distribution in the ceramic and polymer phases at the resonant frequency as a function of the composite thickness as well as the volume fraction of the ceramic phase are obtained, and through the discussion of the vibration field the variation rule of the resonant frequency is well explained. For the resonant frequency the results of the iso-strain model, the stopband resonance model, and the T -matrix model are consistent with the predictions made by this model under the special condition of very fine structure.

I. INTRODUCTION

PIEZOCERAMIC-POLYMER composites have been proven to be efficient and powerful materials for ultrasonic transducers due to their high electro-mechanical coupling and low acoustic impedance [1]. This results in their wide spread acceptance for use in medical and underwater applications. Being a di-phasic material, the characteristics of a composite depend not only on the material parameters of ceramic and polymer phases, but also on their dimensions and operating frequencies. For transducer design, it is important to understand these relationships.

Basically, the previous theoretical works were performed mainly in three directions:

(a) In the case of very fine composite structures, quasistatic and iso-strain approximations were used to derive the effective properties of composites which include the effective elasticity, permittivity, piezoelectricity, and density; hence, the effective acoustic velocities in direction of thickness, the thickness

resonant frequency constant, the effective acoustic impedance, and the effective thickness piezoelectric coupling coefficient [2]–[4]. For an ultrasonic transducer, it is important, but needs to extend the model to the dynamic treatment and include the effect of the finite structure.

(b) By solving for the wave propagation in the direction perpendicular to the thickness in an infinite periodical composite material, the stop band of the wave propagation can be obtained, and the edge of the stop band is related to the lateral periodical resonance of the composite transducers [5]–[7]. The model was also extended to the case of finite thickness by an approximate Lamb wave propagation method [8], [9]. Although the model introduced the useful concept of the stopband edge resonance in a composite structure as the upper limit for the operation frequency range, it does not provide a quantitative and complete description of the lateral periodical resonant modes of a composite.

(c) In addition to the analytical modeling, finite element analysis has been applied to the dynamic problems of the piezo-composite materials [10]–[13]. The results, although very informative, do not proceed with an advancement in concept toward the understanding of dynamic response of the piezo-composites.

The aim of this paper is to develop a model which, beyond the earlier models, can calculate an entire set of dispersion curves for various modes of piezo-composites with 2-2 connectivity. Under certain approximations the thickness resonant frequencies and the lateral periodical resonant frequencies (stop band edge frequencies) appear as two branches of the dispersion curves, expressed as a function of the volume fraction of the ceramic phase (or polymer phase) and the aspect ratio (the ratio of the thickness to the width) of ceramics or polymers.

We will first derive the model by solving the coupled dynamic elastic equations in Section II for an infinitely extended 2-2 composite. From the solution, the dispersion curves as well as the vibration field distribution for each resonant mode are obtained. In Section III the experiments are described. The experimental thickness resonant frequencies and lateral resonant frequencies coincide with the theoretical dispersion curves. Section IV illustrates the rules of the variation of thickness resonant frequencies and lateral resonant frequencies with the thickness and the volume fraction, and explains these variation rules by means of the vibration field distribution. Finally, we compare the results with the earlier models in Section V. We will show that the results of resonant frequency by the iso-strain model, the stopband resonance model, and the T -matrix

Manuscript received July 13, 1994; revised November 28, 1994. This work was supported by the Office of Naval Research under contract N00014-93-0340.

Y. Shui is with Nanjing University, Institute of Acoustics, Nanjing 210093, P. R. China.

X. Geng and Q. M. Zhang are with the Material Research Laboratory, Pennsylvania State University, University Park, PA 16802 USA.

IEEE Log Number 9409993.

model are consistent with the predictions made by this model under special condition of very fine structure.

II. THEORY

For a piezo-composite with 2-2 connectivity, as shown in Fig. 1, we solve for the solutions of waves propagating parallel to the interfaces, i.e., in x_3 direction. Here, we assume that the dimension of the composite in the x_2 direction is large enough that the derivative of all the quantities with respect to x_2 vanishes. For simplicity, we take the piezoelectric ceramic as a nonpiezoelectric, isotropic material in the calculation. This approximation introduces a small error to the resonant frequency, but does not change the main feature of the dispersion curves in the common used range.

Similar to the solution of Lamb wave by using partial waves [14], the plane wave solution propagating in the x_3 direction can be written as

$$\begin{aligned}
 u_1^c &= \left\{ \begin{aligned} &A_{L+}^c \frac{k_{L1}^c}{k_L^c} \exp(ik_{L1}^c x_1) - A_{L-}^c \frac{k_{L1}^c}{k_L^c} \\ &\cdot \exp(-ik_{L1}^c x_1) + A_{T+}^c \frac{k_3^c}{k_T^c} \exp(ik_{T1}^c x_1) \\ &+ A_{T-}^c \frac{k_3^c}{k_T^c} \exp(-ik_{T1}^c x_1) \end{aligned} \right\} \\
 &\cdot \exp(ik_3 x_3 - i\omega t) \\
 u_3^c &= \left\{ \begin{aligned} &A_{L+}^c \frac{k_3^c}{k_L^c} \exp(ik_{L1}^c x_1) + A_{L-}^c \frac{k_3^c}{k_L^c} \\ &\cdot \exp(-ik_{L1}^c x_1) - A_{T+}^c \frac{k_{T1}^c}{k_T^c} \exp(ik_{T1}^c x_1) \\ &+ A_{T-}^c \frac{k_{T1}^c}{k_T^c} \exp(-ik_{T1}^c x_1) \end{aligned} \right\} \\
 &\cdot \exp(ik_3 x_3 - i\omega t) \\
 u_1^p &= \left\{ \begin{aligned} &A_{L+}^p \frac{k_{L1}^p}{k_L^p} \exp(ik_{L1}^p x_1) - A_{L-}^p \frac{k_{L1}^p}{k_L^p} \\ &\cdot \exp(-ik_{L1}^p x_1) + A_{T+}^p \frac{k_3^p}{k_T^p} \exp(ik_{T1}^p x_1) \\ &+ A_{T-}^p \frac{k_3^p}{k_T^p} \exp(-ik_{T1}^p x_1) \end{aligned} \right\} \\
 &\cdot \exp(ik_3 x_3 - i\omega t) \\
 u_3^p &= \left\{ \begin{aligned} &A_{L+}^p \frac{k_3^p}{k_L^p} \exp(ik_{L1}^p x_1) + A_{L-}^p \frac{k_3^p}{k_L^p} \\ &\cdot \exp(-ik_{L1}^p x_1) - A_{T+}^p \frac{k_{T1}^p}{k_T^p} \exp(ik_{T1}^p x_1) \\ &+ A_{T-}^p \frac{k_{T1}^p}{k_T^p} \exp(-ik_{T1}^p x_1) \end{aligned} \right\} \\
 &\cdot \exp(ik_3 x_3 - i\omega t)
 \end{aligned}
 \quad \left. \begin{array}{l} md - \frac{d_c}{2} \leq x_1 \leq md + \frac{d_c}{2} \\ md + \frac{d_c}{2} \leq x_1 \leq md + \frac{d_c}{2} + d_p \end{array} \right\} \quad (1)$$

where m is an arbitrary integer, d_c and d_p are the widths of ceramic plate and polymer plate, $d = d_c + d_p$ is therefore the period. And the volume fraction of the ceramic phase is

$$r = d_c/d$$

u_1^c, u_3^c, u_1^p , and u_3^p are the elastic displacement components in ceramic and polymer regions, respectively, $A_{L+}^c, A_{L-}^c,$

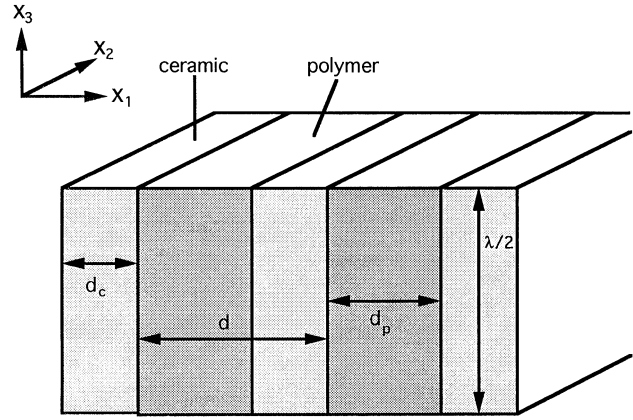


Fig. 1. The schematic diagram of a 2-2 composite.

$A_{T+}^c, A_{T-}^c, A_{L+}^p, A_{L-}^p, A_{T+}^p,$ and A_{T-}^p are the amplitudes of longitudinal and transverse partial waves, $k_L^c, k_T^c, k_L^p,$ and k_T^p are the moduli of the corresponding wave vectors which have a common component k_3 in the x_3 -direction, and have $k_{L1}^c, k_{T1}^c, k_{L1}^p,$ and k_{T1}^p as their respective x_1 -components. k_{L1} and k_{T1} for both ceramic and polymer are given by

$$\begin{aligned}
 k_{L1} &= \sqrt{k_L^2 - k_3^2}, \quad k_{T1} = \sqrt{k_T^2 - k_3^2} \\
 \omega &= k_L v_L = k_T v_T
 \end{aligned} \quad (2)$$

where v_L and v_T are the velocities of longitudinal and shear waves.

For a composite transducer, only the symmetrical modes are piezo-electric active. In most cases of transducer application only the symmetrical modes are concerned. Substitute the symmetrical conditions

$$\begin{aligned}
 u_1^c(x_1) &= -u_1^c(-x_1), \\
 u_3^c(x_1) &= u_3^c(-x_1) \\
 u_1^p\left(x_1 - \frac{d}{2}\right) &= -u_1^p\left(\frac{d}{2} - x_1\right) \\
 u_3^p\left(x_1 - \frac{d}{2}\right) &= u_3^p\left(\frac{d}{2} - x_1\right)
 \end{aligned} \quad (3)$$

into (1), one can have

$$\begin{aligned}
 A_{L+}^c &= A_{L-}^c, \quad \text{put} = A_L^c/2 \\
 A_{T+}^c &= -A_{T-}^c, \quad \text{put} = A_T^c/2 \\
 A_{L+}^p &= A_{L-}^p, \quad \text{put} = A_L^p/2 \\
 A_{T+}^p &= -A_{T-}^p, \quad \text{put} = A_T^p/2
 \end{aligned}$$

then (1) becomes

$$\begin{aligned}
 u_1^c &= i \left\{ \begin{aligned} &A_L^c \frac{k_{L1}^c}{k_L^c} \sin(k_{L1}^c x_1) \\ &+ A_T^c \frac{k_3^c}{k_T^c} \sin(k_{T1}^c x_1) \end{aligned} \right\} \\
 &\cdot \exp(ik_3 x_3 - i\omega t) \\
 u_3^c &= \left\{ \begin{aligned} &A_L^c \frac{k_3^c}{k_L^c} \cos(k_{L1}^c x_1) \\ &- A_T^c \frac{k_{T1}^c}{k_T^c} \cos(k_{T1}^c x_1) \end{aligned} \right\} \\
 &\cdot \exp(ik_3 x_3 - i\omega t)
 \end{aligned}$$

$$\begin{aligned}
& -\frac{d_c}{2} \leq x_1 \leq \frac{d_c}{2} \\
u_1^p = & \left. i \left\{ A_L^p \frac{k_{L1}^p}{k_L^p} \sin \left[k_{L1}^p \left(x_1 - \frac{d}{2} \right) \right] \right. \right. \\
& \left. \left. + A_T^p \frac{k_3^p}{k_T^p} \sin \left[k_{T1}^p \left(x_1 - \frac{d}{2} \right) \right] \right\} \right. \\
& \left. \cdot \exp(ik_3 x_3 - i\omega t) \right. \\
u_3^p = & \left. \left\{ A_L^p \frac{k_3^p}{k_L^p} \cos \left[k_{L1}^p \left(x_1 - \frac{d}{2} \right) \right] \right. \right. \\
& \left. \left. - A_T^p \frac{k_{T1}^p}{k_T^p} \cos \left[k_{T1}^p \left(x_1 - \frac{d}{2} \right) \right] \right\} \right. \\
& \left. \cdot \exp(ik_3 x_3 - i\omega t) \right. \\
& \left. \frac{d_c}{2} \leq x_1 \leq \frac{d_c}{2} + d_p. \right. \quad (4)
\end{aligned}$$

It expresses the solution in one unit cell among all periodically repeated cells.

The boundary conditions at the ceramic-polymer interface are

$$\begin{aligned}
u_3^c \left(\frac{rd}{2} \right) &= u_3^p \left(\frac{rd}{2} \right) \\
u_1^c \left(\frac{rd}{2} \right) &= u_1^p \left(\frac{rd}{2} \right) \quad (5a)
\end{aligned}$$

$$\begin{aligned}
T_{11}^c \left(\frac{rd}{2} \right) &= T_{11}^p \left(\frac{rd}{2} \right) \\
T_{13}^c \left(\frac{rd}{2} \right) &= T_{13}^p \left(\frac{rd}{2} \right). \quad (5b)
\end{aligned}$$

The stress components are related to the strain components in an isotropic material by

$$\begin{aligned}
T_{11} &= c_{11} \frac{\partial u_1}{\partial x_1} + c_{12} \frac{\partial u_3}{\partial x_3} \\
T_{13} &= c_{44} \left(\frac{\partial u_1}{\partial x_3} + \frac{\partial u_3}{\partial x_1} \right). \quad (6)
\end{aligned}$$

Substituting (4) into boundary conditions (5) yields the following linear equations which relate the four unknown amplitudes in (4), i.e., $A_L^c, A_T^c, A_L^p,$ and A_T^p

$$\begin{bmatrix} K_{11} & K_{12} & K_{13} & K_{14} \\ K_{21} & K_{22} & K_{23} & K_{24} \\ K_{31} & K_{32} & K_{33} & K_{34} \\ K_{41} & K_{42} & K_{43} & K_{44} \end{bmatrix} \begin{bmatrix} A_L^c \\ A_T^c \\ A_L^p \\ A_T^p \end{bmatrix} = 0. \quad (7)$$

Here, we give one example for the expression of K elements:

$$K_{41} = -c_{44}^c \frac{2k_3 k_{L1}^c}{k_L^c} \sin \left(k_{L1}^c \frac{rd}{2} \right).$$

The condition of a nonzero solution for $A_L^c, A_T^c, A_L^p,$ and A_T^p requires that the determinant of the matrix $[K_{ij}]$ equals zero, where all the matrix elements are functions of frequency ω and wave vector k_3 . From (7), one can solve for the relationship between ω and k_3 which presents as the dispersion curves of the wave propagating in the composites along the x_3 axis. For each pair of ω and k_3 , there is a solution set of ratios between the amplitudes $A_L^c, A_T^c, A_L^p,$ and A_T^p from (7). Substitute them into (4), the vibration distribution in the two phases for that mode is then obtained.

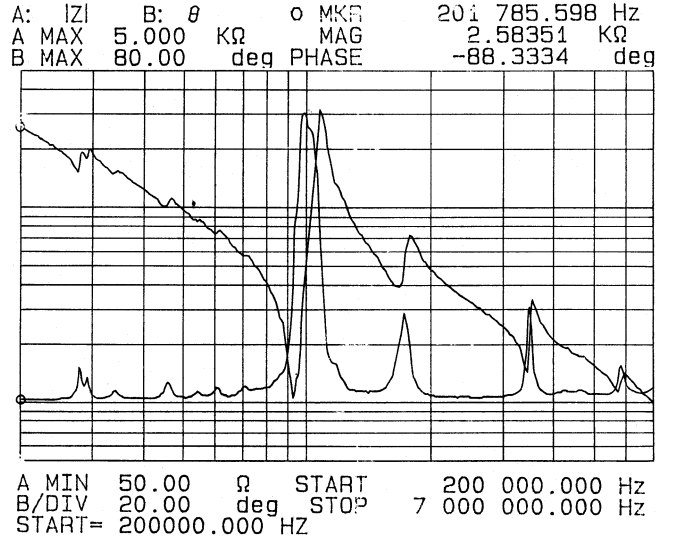


Fig. 2. The measured electrical impedance curve of a composite transducer. The length, width, and thickness of the transducer are 13.77, 6.37, and 1.56 mm, respectively. The widths of ceramic and polymer plates are 0.35 and 0.28 mm, respectively.

In order to model a 2-2 composite transducer with a finite thickness, we assume that at resonance the wavelength λ_3 in the x_3 direction is twice the transducer thickness t , hence $k_3 = 2\pi/\lambda_3 = \pi/t$. Here by ignoring mode coupling effects at the two end faces of the transducer, some error will be introduced. It will be serious as the transducer becomes too thin (in estimation when the polymer aspect ratio t/d_p is smaller than one, $d_p/t = 2d_p/\lambda_3 = 2(1-r)d/\lambda_3 > 1$, the deviation might become obvious).

III. EXPERIMENTS

To compare with the theoretical results, a series of 2-2 composites were fabricated with different thicknesses and ceramic volume fractions. These composites were made by PZT-5H and Spurs epoxy with density 1080 kg/m³. The longitudinal and shear velocities of the epoxy measured by the time-of-flight technique are 2.20 and 1.07 km/s, respectively. In all these composites, the polymer width d_p was fixed at 0.35 mm. The electrical impedance of the transducer was measured by a HP impedance analyzer (model 4191A). A typical impedance curve measured from a 2-2 composite sample with ceramic volume fraction $r = 0.45$ and thickness $t = 1.56$ mm is presented in Fig. 2. From the relevant velocities of the two phases as well as the characteristic of the measured impedance curve, the resonance modes can be identified. For example, the thickness mode is distinguished from other modes by the large piezoelectric coupling, the difference between resonant and anti-resonant frequencies for the thickness mode is larger than the other modes. In Fig. 2, the thickness resonant and anti-resonant frequencies of this composite are 0.918 and 1.089 MHz, while the third and fifth harmonics are at 3.546 and 5.98 MHz, respectively. The resonance mode at 1.76 MHz is related to the lateral resonance of the composite periodic structure.

TABLE I
THE PARAMETERS OF CERAMIC AND EPOXY USED IN CALCULATION

c_{11}^c	c_{44}^c	c_{11}^p	c_{44}^p	ρ^c	ρ^p
(10^{10}N/m^2)	(10^{10}N/m^2)	(10^{10}N/m^2)	(10^{10}N/m^2)	(10^3kg/m^3)	(10^3kg/m^3)
13.9	4.0	0.53	0.13	7.5	1.1

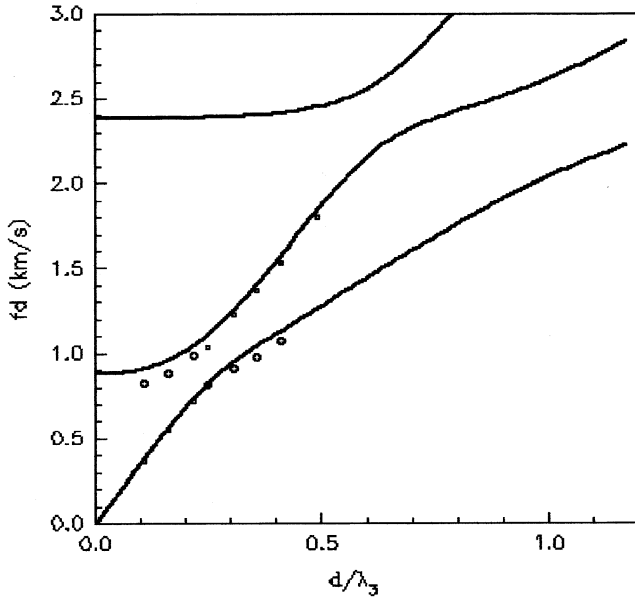


Fig. 3. The dispersion curves of waves propagating in a 2-2 PZT-5H-Spurs epoxy composite transducer for volume fraction of ceramic $r = 0.3$. The frequency f and the wavelength λ_3 are normalized by the period of composite d . The theoretical curves are solid lines and the experimental data are marked as circles. The smaller circles are the thickness resonance.

IV. RESULTS AND DISCUSSIONS

As an example, Fig. 3 illustrates the calculated dispersion curves of $r = 0.3$ (solid line) with the corresponding experimental data of antiresonant frequencies (circles). The experimental thickness modes are expressed by smaller circles. In the calculation, the parameters used for the ceramic phase are rounded to isotropic ones approximately from those of PZT-5H ceramic. The parameters of epoxy are taken from the measurements of the samples. All the parameters for both the polymer and approximate isotropic ceramic phases are listed in Table I. They are used in all the calculations presented in this paper.

One can predict the dependence of thickness and lateral resonant frequencies on the thickness and volume fraction from the corresponding dispersion curve. This is of great interests in the practical applications.

At large thickness ($d/\lambda_3 \approx d/2t \ll 1$) the thickness mode and the lateral resonance mode correspond to the lowest and second curve of the dispersion curves in Fig. 3, respectively. The third curve we will discuss at the end of this session. The dependence of the thickness resonant frequency on the thickness t at large thickness is nearly a straight line (the beginning

portion of the lowest curve in Fig. 3). Since in such case the composite structure is fine (period $d \ll$ wavelength λ_3), the wave velocity v_3 in the thickness direction ($v_3 = f\lambda_3$ is the slope of the curve) changes very little with x_3 -wavelength $\lambda_3 = 2t$. In the same region of d/λ_3 the lateral resonant frequency varies slightly with thickness. As the value of d/λ_3 increases, the thickness resonant frequency approaches that of the lateral periodical resonant frequency, the mode coupling between two modes occurs as has been indicated in principle [15].

Replacing d by d_p , we redraw the dispersion curves for various ceramic volume fractions r , and put them together in Fig. 4. For $r = 0.7$, the mode coupling between the thickness and lateral modes is very weak since the fundamental and second curves almost intersect at a point. As r decreases from 0.7 to 0.3, the coupling between modes becomes stronger, and two curves shift apart from each other. As the thickness is thinner, the portion of second curve after mode coupling region looks like the extension of the beginning part of the lowest curve, vice versa, the portion of lowest curve after mode coupling region seems to be the extension of the second curve before mode coupling region. The experimental thickness resonant frequencies plotted in Fig. 3 (small circles) which we identified by the strong piezoelectric coupling, are close to the second curve after the mode coupling region and follow the lowest curve before the mode coupling region. It reflects that the piezoelectric coupling coefficient is changing with the thickness for both the modes.

We found both experimentally and theoretically, that for 2-2 piezo-composites in case of large aspect ratio of the polymer (t/d_p), the lateral periodical resonant frequency in an appropriate range of volume fraction is mainly determined by the width of polymer d_p , other than the whole period d . In Fig. 3, the second curve at small d/λ_3 represents the lateral periodical resonant frequency. We plot the lateral resonant frequency at zero d/λ_3 versus ceramic volume fraction r , as shown in Fig. 5. In Fig. 5 the frequency is normalized by the period d . If the width of polymer d_p is used instead of d to normalize the frequency f , we have Fig. 6. It is clear from Fig. 6 that in the region of $0.2 < r < 0.75$, the curve is rather flat (fd_p ranges from 3.69 to 3.33, $\Delta f/f < 5\%$). It could be well explained by the field distribution of the wave.

Fig. 7 shows a typical field distribution (relative amplitude profile of displacement $u_3(x_1)$ in the x_3 -direction) for the lateral mode of $r = 0.3$ and $d/\lambda_3 = 0.03$ at $fd = 0.880$ MHz/mm. The sign of the vibration in ceramic is opposite to the sign over most area of polymer, so the vibration in ceramic

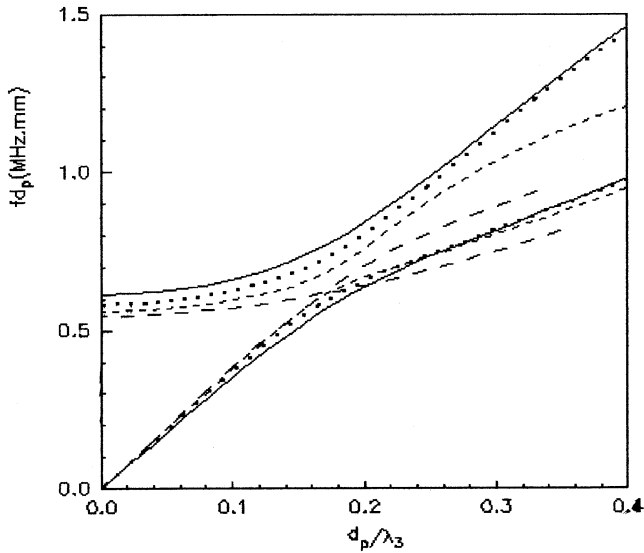


Fig. 4. The dispersion curves for various volume fraction of ceramic r , normalized by the width of polymer d_p . Solid line, $r = 0.3$; dotted line, $r = 0.45$; short dashed line, $r = 0.6$; dashed line, $r = 0.7$.

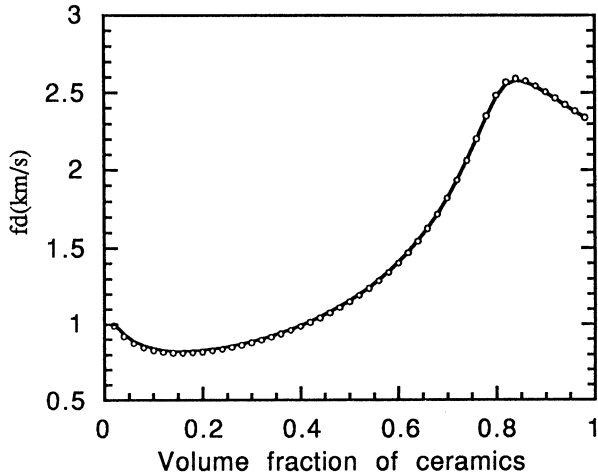


Fig. 5. The lateral periodic resonant frequency f of composite transducers at $d/\lambda_3 \rightarrow 0$ limit for various volume fraction of ceramic r . f is normalized by the period d . Solid line is calculated from the dynamic model, circles are from the T -matrix method.

is out-of-phase to that in polymer. At zero d/λ_3 , $A_L^c = A_L^p = 0$, $k_3 \rightarrow 0$, $k_{T1}^c \rightarrow k_T^c$, $k_{T1}^p \rightarrow k_T^p$, the lateral mode is a periodically combined pure shear wave resonance in the lateral direction. According to (4) the amplitude distributions are cosine curves both in polymer and ceramic, respectively. Since $(k_T^c/k_T^p) = (v_T^p/v_T^c)$, the ratio of total argument of cosine curves in polymer to that in ceramic is $[rk_T^c/(1-r)k_T^p] = [rv_T^p/(1-r)v_T^c]$. At $r \approx 0.7$ the ratio is close to 1, both of the arguments in polymer and ceramic are nearly π , the vibration in each polymer and ceramic plate behaves as an independent resonance. This is the reason of weak mode coupling in such case. Under the critical ceramic volume fraction value r_0 satisfying the condition $[r_0v_T^p/(1-r_0)v_T^c] = 1$, fd_p of lateral periodical resonance must be equal to the half of polymer shear velocity $v_T^p/2$ (the same for ceramic $fd_c = v_T^c/2$). From the stress continuity boundary condition, because the shear elastic stiffness of polymer is much smaller than that of

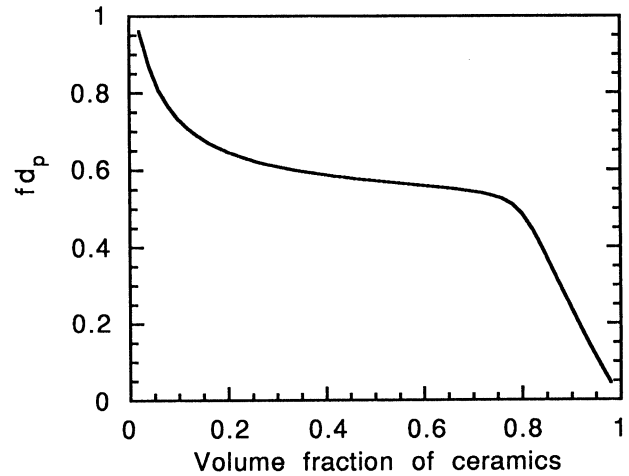


Fig. 6. The same curve as in Fig. 5, but f is normalized by the width of polymer d_p .

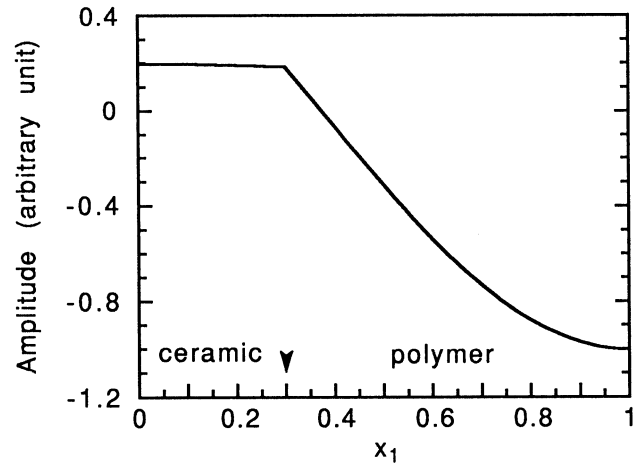


Fig. 7. The vibration amplitude distribution at the lateral periodic resonance of composite for $r = 0.3$ and $d/\lambda_3 = 0.03$.

ceramic (in our calculation they are 0.13 and 4.0, respectively), the amplitude at the center of polymer would be much larger than in ceramic, as shown in Fig. 7. In case of ceramic volume fraction value smaller than r_0 , since the amplitude difference is large, the reduction of volume fraction value causes a small increment to the total argument of cosine curve in polymer from π due to the displacement continuity condition. This explains that there is only a little raise of fd_p as r is reduced from 0.7 to 0.3. The larger is the acoustic impedance difference between polymer and ceramic, the weaker is the growth of fd_p from the weak coupling point. This rule allows one to estimate the lateral resonant frequency with moderate ceramic volume fraction r at small d/λ_3 . In an extreme case, suppose the acoustic impedance ratio between polymer and ceramic approaches zero, the vibration in polymer would become a clamped shear wave resonance and the resonant frequency would be always $v_T^p/2d_p$, no matter with the volume fraction.

In experiments we have noticed that the widths between two zero surface vibration positions in polymer, observed by a ultra-dilatometer laser probe, are narrower than the widths of polymer plates for the second modes. It is consistent with the theoretical analysis.

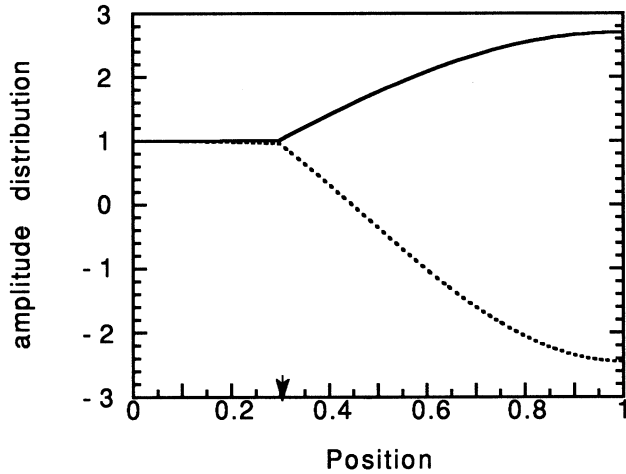


Fig. 8. The vibration amplitude distribution at the first (solid line) and second (dashed line) modes of wave in composite for $r = 0.3$ and $d/\lambda_3 = 0.24$.

For the thickness resonance at small d/λ_3 the x_3 component vibration amplitude distribution across the whole unit is about a constant and there is almost no x_1 vibration component, similar to the thickness resonance of an transducer made by homogeneous material. With the decrease of thickness, the x_3 -component of vibration in polymer becomes stronger than that in ceramic, the field distribution has a ripple in each unit even though at thickness resonance as the optical probe measurement on the 1-3 composite has demonstrated [5], [6].

Fig. 8 shows a typical vibration amplitude distribution in ceramic and polymer for both thickness and lateral modes with $r = 0.3$ and $d/\lambda_3 = 0.24$ at resonant frequencies 0.80 and 1.09 MHz, respectively, within the region of mode coupling between thickness and lateral modes. The amplitudes are normalized to the amplitude at the center of ceramic. In order to show the vibration field variation with the thickness, Fig. 9 illustrates the ratio between the amplitudes at the center of polymer and that at the center of ceramic for $r = 0.3$. For the mode corresponding to the lowest curve in Fig. 3, this ratio increases with the decrease of the composite thickness which means there would be more ripple at the surface for thinner (relative to lateral period) transducer. The vibrations of ceramic and polymer for the mode on the lowest curve are always in-phase as the amplitude ratio is always positive. Vice versa, for the mode on the second curve, the ratio is negative, there would always be a significant ripple at the surface. As shown in Fig. 3, when the d/λ_3 value is above the mode coupling region, the thickness resonant frequency is on the upper branch of the Fig. 3 dispersion curves, in this case the polymer and ceramic oscillate out-of-phase at the thickness resonance. For high frequency operation, due to the limitations of fine scale dicing technology, one has to fabricate the transducers operating at a rather large value of $d/2t (=d/\lambda_3)$, compromising the uniformity of surface vibration. One should note that the above discussions apply to the free surfaces of the transducers, and in practical cases there are often acoustic loads on both sides which will alter things. The resonance with strong piezoelectric coupling switches from the mode on the lowest curve before mode coupling region to the mode on the second curve after mode coupling region, but the resonant

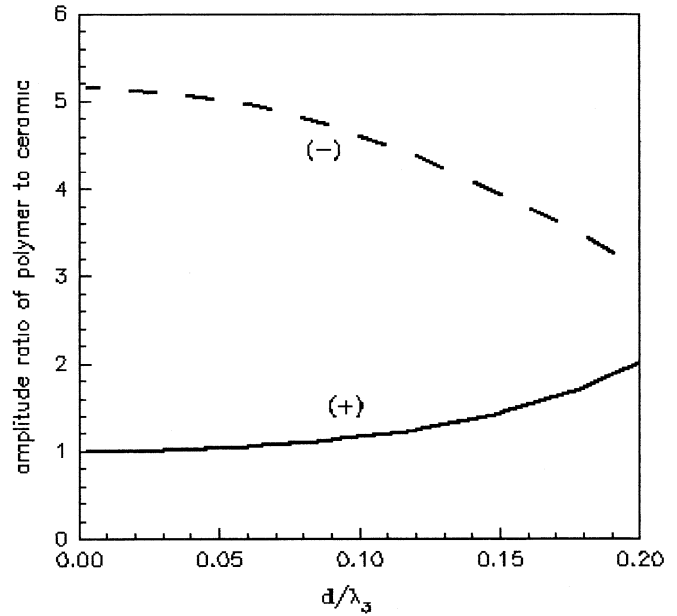


Fig. 9. The ratio of amplitudes at the center of polymer to that at the center of ceramic versus d/λ_3 for $r = 0.3$. Solid line is for the first mode and dotted line is for the second mode.

frequencies of both the modes are changing continuously, and the variation of their vibration field are continuous as well.

In Fig. 3 only three curves are illustrated. In fact, there are infinite branches of dispersion curves as we extend the figure to higher values of the ordinate. The third curve in Fig. 3 represents the lateral third harmonic resonance, at which the vibration in polymer is about one and half periods instead of half period in the second mode. In Fig. 4, we omitted the higher mode for clarity.

V. COMPARISON WITH OTHER MODELS

1) *The Iso-strain Model*: The iso-strain model provide a good approximation for the thickness resonance of long wavelength relative to period d [2]–[4]. In order to compare the dynamic model with iso-strain model, we derived an effective stiffness formulae for a nonpiezoelectric isotropic 2-2 composite according to the principle used by W. Smith *et al.* for 1-3 composite [2], [3]

$$\begin{aligned} \bar{\rho} &= r\rho^c + (1-r)\rho^p \\ \bar{c}_{33} &= rc_{11}^c + (1-r)c_{11}^p - \frac{r(1-r)(c_{12}^c - c_{12}^p)^2}{rc_{11}^p + (1-r)c_{12}^c} \end{aligned} \quad (8)$$

The effective longitudinal wave velocity in the x_3 direction can be derived from these formulae. For the dynamic model, the wave velocity can be obtained from the slope at the origin of the lowest dispersion curve for various volume fraction r . Comparing the two models, the two curves coincide exactly as shown in Fig. 10. Therefore, for the thickness resonant frequency the iso-strain model describes the special case of small d/λ_3 in the lowest dispersion curve of the dynamic model.

2) *The Stopband Resonance Model* [5],[6]: The stopband resonance model addressed the lateral period resonance as the stop band edge of the wave propagation in direction perpendicular to the interfaces of the ceramic and polymer. In dynamic model, part of the second mode (before the mode

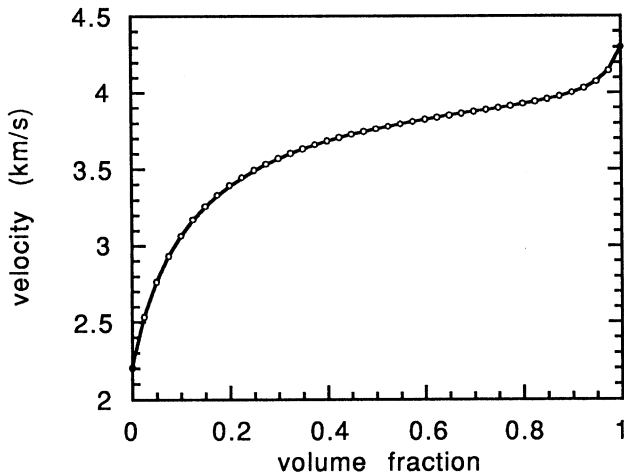


Fig. 10. The wave velocity of composite along the x_3 direction for $r = 0.3$ and $d/\lambda_3 \rightarrow 0$. The solid line represents the result of the dynamic model and the circles are from iso-strain model.

coupling) is related to the lateral periodical resonance. In case of $d/\lambda_3 \rightarrow 0$, the resonant frequency of stop band mode can be calculated by the T -matrix method which considers the shear wave propagation in the direction perpendicular to the interfaces of the ceramic and polymer. In the T -matrix method each plate, either a ceramic or a polymer one, is equivalent to a transmission line, mathematically expressed by a matrix, and the whole composite can be represented as the combination of ceramic and polymer transmission matrices in alternative series connection. Combining two of them as a unit cell, the propagation phase θ of a unit cell (a period) can be derived by ordinary matrix technique

$$\cos \theta = \cos \frac{\omega d_c}{v_T^c} \cos \frac{\omega d_p}{v_T^p} - \frac{1}{2} \left(\frac{Z_c}{Z_p} + \frac{Z_p}{Z_c} \right) \sin \frac{\omega d_c}{v_T^c} \sin \frac{\omega d_p}{v_T^p} \quad (9)$$

where $Z_c = \rho^c v_T^c$ and $Z_p = \rho^p v_T^p$ are the acoustic impedance of ceramic and polymer. The stop band is determined by $\cos \theta \geq 1$, and the stop band edge corresponds to $\cos \theta = 1$. The frequency of the upper edge in the two solutions of $\cos \theta = 1$ is for the lateral resonant frequency in the symmetrical case. The results of stop band edge frequency calculated from (9) for various ceramic volume fraction r are plotted in Fig. 5 combined with the frequencies of the second dispersion curve at zero d/λ_3 by the dynamic model. They overlap each other. We can therefore conclude that the stopband model describes the zero d/λ_3 case of the dynamic model for lateral modes.

VI. SUMMARY

In this paper we developed a dynamic model, which can quantitatively describe both the thickness and lateral resonant modes of 2-2 composites with respect to the aspect ratio and volume fraction. In certain ranges of volume fraction, the width of the polymer plays a dominant role in determining the lateral periodical resonant frequency at large aspect ratio of polymer. The vibration field distributions in both ceramic and polymer for various thickness are analyzed, and through the discus-

sion of vibration distribution a physical interpretation for the behavior of the dispersion curves is given. The surface vibration ripple of the thickness mode is related to the aspect ratio.

The dynamic model represents a method to solve the dynamic problems of periodic composite transducers. However, what we have done in this paper is just a preliminary work. By taking the composite thickness as half a wavelength in x_3 -direction, the effect of the end faces is neglected. As the further works to do, the piezoelectricity will be put into this model to study the dependence of the piezoelectric coupling coefficient k_t on the aspect ratio and volume fraction. The end face approximation will be corrected and, then, all the backing material, acoustic loading, and/or the matching layer will be included in the considerations. This model also needs to be extended to 1-3 composite so as to better satisfy practical design requirements.

ACKNOWLEDGMENT

The authors would like to thank Mr. W. K. Qi, Dr. H. Kunkel, Dr. J. Yuan, Prof. Wenwu Cao, and E. Cross for their help in this work. We are obliged to Dr. Suwen Wang for his literal revision of this article.

REFERENCES

- [1] T. R. Gururaja, W. A. Schulze, L. E. Cross, R. E. Newnham, B. A. Auld, and Y. J. Wang, "Piezoelectric composite materials for ultrasonic transducer applications, Part I: Resonant modes of vibration of PZT rod-polymer composites," *IEEE Trans. Sonic and Ultrasonics*, vol. SU-32, pp. 481-497, 1985.
- [2] W. A. Smith, A. Shaulov, and B. A. Auld, "Tailoring the properties of composite piezoelectric materials for medical ultrasonic transducers," in *Proc. 1985 IEEE Ultrason. Symp.*, pp. 642-647.
- [3] W. A. Smith and B. A. Auld, "Modeling 1-3 composite piezoelectrics: Thickness-mode oscillations," *IEEE Trans. Ultrason., Ferroelect., Freq. Cont.*, vol. 38, pp. 40-47, 1991.
- [4] K. Y. Hashimoto and M. Yamaguchi, "Elastic, Piezoelectric and dielectric properties of composite materials," in *Proc. 1986 IEEE Ultrason. Symp.*, 1986, pp. 697-702.
- [5] B. A. Auld, Y. Shui, and Y. Wang, "Elastic wave propagation in three-dimensional periodic composite materials," *J. Physique*, vol. 45, pp. 159-163, 1983.
- [6] B. A. Auld, H. A. Kunkel, Y. Shui, and Y. Wang, "Dynamic behavior of periodic piezoelectric composites," in *Proc. 1983 IEEE Ultrason. Symp.*, pp. 554-558.
- [7] T. R. Gururaja, W. A. Schulze, L. E. Cross, R. E. Newnham, B. A. Auld, Y. Shui, and Y. Wang, "Resonant modes of vibration in piezoelectric PZT rod-polymer composite with two dimensional periodicity," *Ferroelect.*, vol. 54, pp. 183-186, 1984.
- [8] B. A. Auld and Y. Wang, "Acoustic wave vibrations in periodic composite planes," in *Proc. 1984 IEEE Ultrason. Symp.*, 1984, pp. 528-532.
- [9] Y. Wang and B. A. Auld, "Acoustic wave propagation in one-dimensional periodic composites," in *Proc. 1985 IEEE Ultrason. Symp.*, 1985, pp. 637-641.
- [10] A.-C. Hladky-Hennion and J.-N. Decarpigny, "Finite element modeling of active periodic structures: Application to 1-3 piezocomposites," *J. Acoust. Soc. Am.*, vol. 94, no. 2, pp. 621-635, 1993.
- [11] J. Bennett, R. Hamilton, and G. Hayward, "Finite element modeling of 1-3 composite transducers for underwater applications," in *Proc. 1993 IEEE Ultrasonics Symp.*, 1993, pp. 1113-1116.
- [12] P. Challande, "Optimizing ultrasonic transducers based on piezoelectric composites using finite-element method," *IEEE Trans. Ultrason., Ferroelect., Freq. Cont.*, vol. 37, no. 2, pp. 135-140, 1990.
- [13] J. A. Hossack and G. Hayward, "Finite-element analysis of 1-3 composite transducers," *IEEE Trans. Ultrason., Ferroelect., Freq. Cont.*, vol. 38, no. 6, pp. 618-629, 1991.
- [14] B. A. Auld, *Acoustic Fields and Waves in Solids*. New York: Wiley, 1973, vol. 2, p. 78.

- [15] F. Craciun, L. Sorba, E. Morinari, and M. Pappalardo, "A coupled mode theory for periodic piezoelectric composites," *IEEE Trans. Ultrason., Ferroelect., Freq. Cont.*, vol. 36, no. 1, pp. 50–55, 1989.



Yongan Shui graduated from the Physics Department, Beijing University, Beijing, China in 1953.

He is Professor of Acoustics, Nanjing University, Nanjing, China, and has been a visiting scientist at Ginton Laboratory, Stanford University, Stanford, CA, from 1982 to 1983, a Research Professor at Polytechnic Institute of New York, in 1983, an Invited Professor at Paris sixth University from 1987 to 1988 and a Visiting Professor at Materials Research Laboratory, Penn State University, PA, from 1993 to 1994.

Mr. Shui is a fellow of Chinese Acoustical Society. He has been working on surface acoustic wave, ultrasonic transducers, acoustic nonlinear effects, and published about 60 papers. He received the science and technology prizes from Chinese State Educational Bureau, Educational Bureau of Jiangsu Province, China and Chinese Ministry of Electronics eight times.

Xuechang Geng, photograph and biography not available at the time of publication.

Q. M. Zhang received the B.S. degree in physics from Nanjing University, China, in 1981 and the Ph.D. degree in physics from the Pennsylvania State University, University Park, in 1986.

He is currently an Associate Professor of Materials and Senior Research Associate at the Intercollege Materials Research Laboratory of the Pennsylvania State University. His research interests involve piezoceramic and polymer for actuator, sensor, and transducer applications; new design and modeling of piezocomposites; smart materials and structures; novel, artificial, and nano-composite materials; effect of defect structure on the dielectric, piezoelectric, and elastic properties of ferroelectric materials; and structural studies on interfaces and defects in ferroelectrics. From 1986 to 1988, he was a Post Doctoral researcher at the Materials Research Laboratory of Penn State University. From 1988 to 1991 he was a research Scientist at Brookhaven National laboratory, NY, conducting research on interface, surface, and thin films with neutron and synchrotron X-ray scattering techniques.

Dr. Zhang is a member of the American Ceramic Society, American Physical Society, and Neutron Scattering Society of America.